Beam-like damage detection methodology using wavelet damage ratio and additional roving mass

Juliana C. Santos, Marcus V. G. de Morais, Marcela R. Machado, Ramon Silva
University of Brasilia, Brazil
julianasaaantos@gmail.com, https://orcid.org/0000-0003-0459-8655,
mvnorais@unb.br, https://orcid.org/0000-0003-4800-4513,
marcelam@unb.br, https://orcid.org/0000-0002-7488-7201
ramon.silva@unb.br, https://orcid.org/0000-0003-2004-6236

Erwin U. L. Palechor
Federal University of Cariri, Brazil
erwinlopezpalechor@hotmail.com, https://orcid.org/0000-0003-1409-1882

Welington V. Silva
University of Brasilia, Brazil
welington.vital@gmail.com, https://orcid.org/0000-0001-5200-5995

ABSTRACT. Early damage detection plays an essential role in the safe and satisfactory maintenance of structures. This work investigates techniques that use only damaged structure responses. A Timoshenko beam was modeled in finite element method, and an additional mass was applied along their length. Thus, a frequency-shift curve is observed, and different damage identification techniques were used, such as the discrete wavelet transform and the derivatives of the frequency-shift curve. A new index called wavelet damage ratio (WDR) was defined as a metric to measure the damage levels. Damages were simulated like a mass discontinuity (mass damage). It was evaluated for different damage levels and positions. Numerical results showed that all proposed techniques are efficient for damage identification in Timoshenko beams with low computational cost and practical application.

KEYWORDS. Structural Health Monitoring; Damage detection; Timoshenko beam; Frequency-shift; Wavelet; Additional Roving Mass.

INTRODUCTION

E arly damage detection plays a vital role in the safe and satisfactory maintenance [1]. Structural damage is any punctual or generalized change in the structure material or geometric properties that may affect the durability. In practice, it is difficult to recognize most damages by using visual inspection techniques, for instance, in cases that

damage is in a position that is difficult to access. Besides, it can require long analysis time and high cost. In this way, they may be detected by acoustic emission, ultrasonic guided-waves, eddy current detection, liquid penetrant test, magnetic particle inspection, radiographic testing and vibration-based non-destructive techniques [2–9]. System identification is an essential tool for such a purpose. Even if some non-destructive methods require finding other techniques with greater efficiency and lower cost.

Generally, techniques compare the intact and damaged response of the structures, which need the identification of both beforehand. Most of the time, the intact response is very difficult to be obtained. Hence, researchers have been testing some techniques using only the damaged response, as [10–16].

Structural health monitoring (SHM) consists of periodic evaluations, on a full scale, the dynamic behavior of structures using sensors installed in the structural system to detect environmental actions and determine proactive maintenance actions. Non-destructive methods and monitoring techniques have received particular attention among which the vibration analysis for damage detection has been applied for its simplicity of implementation and for presenting parameters sensitive to damage [17–19].

Reviews [17,18] present damage identification techniques based on (a) natural frequency, (b) modal shape, (c) curvature in the modal form, (d) measure of dynamic flexibility, (e) updating, (f) heuristic methods by specialized networks, among others. There are several methodologies in the literature for solving damage detection problems using energy-based techniques [20–29], some based on genetic algorithms [30–35] and elastic wave propagation at medium and high-frequency bands, such [36–39].

Structural damages may have a severe influence on the dynamic characteristics. It produces a local change in stiffness, changing dynamic characteristics such as mass distribution and damping properties. Therefore, reduction in stiffness is associated with decreases in the natural frequencies and modification of the mode shape of the structure [40]. The ease of identification of natural frequencies has motivated the dynamic analysis of cracked structures. Some researchers are focused on the computation of natural frequencies of the cracked structure. Salawu [41] has presented a review of damage detection methods using natural frequencies potentially useful for routine integrity assessment of structures. Frequency values obtained from periodic vibration tests can monitor structural behavior and assess the structural condition. An advantage of the approach is the global nature of the identified frequencies, thus allowing the selected 36 measurement points. Fan and Qiau [19] presented an updated version of the review later. Zhong et al [12,42,43] focused on investigating natural frequencies of cracked beams subjected to a roving mass that is stationary at each location considered. The roving of the mass enhances the crack's effects on the beam dynamics and facilitates the identification and location of damage in the beam.

Researchers have focused on the study of the vibration analysis with auxiliary masses. It consists of crossing the additional mass along the structure to magnify the effect of discontinuities on the dynamic response and, hence, to facilitate the identification and location of damage in structures. Palechor et al. [44] applied this technique using impact force excitation in supported beams and identified frequency perturbation by wavelet transform. Palechor et al. [45] developed a new spectral-element with additional mass and compared the spectral method, and Galerkin assumed-mode with experimental results of an I-shape simply supported beam, presented good experimental agreement with low computational cost. Mahmoud and Abou Zaid [46] have investigated mode shapes of structures, supported and cantilever beams, subjected to a moving mass of a fixed or different velocity. Eun et al. [47] presented the damage detection method using the variation of Frequency Response Function (FRF) measured by moving an additional mass in the structure. The results showed that the FRF curvature method could be used under external noise through a numerical experiment. Solís et al. [48] presented the damage detection methodology based on the wavelet analysis based on the variation in the mode shapes derived from the damage. An additional moving mass was used to emphasize the effect of the damage and reduce experimental noise. Wang et al. [49] presented the frequency-shift to detect local stiffness reduction. The authors claim this technique can be easily adapted to a given problem since the index sensitivity can be adjusted by changing the additional mass or excitation power. Besides, an algorithm was proposed to adjust the frequency and amplitude contribution in the method automatically. Therefore, a procedure based on the Discrete Fourier Transform was explored to extract precise frequency and amplitude. Lee and Eun [50] performed a numerical and experimental analysis in a damaged beam subject to a moving mass and presented that the strain data, the acceleration, the mass magnitude, and the velocity can affect the damage detection's viability.

Damage detection of structures is an exciting field of research, and the use of additional mass is promising. This paper presents a study on an additional mass spatial probing identification technique as a preliminary step to apply Zhong et al. [12] damage identification technique. First of all, a numerical model on the Timoshenko finite element 2-nodes beam by FEM was implemented. Discrete wavelet transform [51] and derivatives of the frequency-shift curve [4] were used to locate the damage. Damages were simulated like a mass discontinuity [52–54]. Both models were correlated to ease future

experimental tests since it is more practical to simulate damage as mass added which does not require the destruction of the sample under study. Also, it was evaluated for different levels and positions of damages, and the results were presented as maps.

TIMOSHENKO BEAM FORMULATION WITH MASS DISCONTINUITY

In the case of free vibration, the motion equation for uniform beams with a roving mass m_a positioned at the damage position L_d is described by [56–58]:

$$
\begin{cases}
\dfrac{\partial}{\partial x}\left[kGA\left(\dfrac{\partial u}{\partial x} - \theta \right) \right] = \left[\rho A + m_a \delta\left(x - L_d \right) \right] \dfrac{\partial^2 u}{\partial t^2} \\
\dfrac{\partial}{\partial x}\left[EI \dfrac{\partial \theta}{\partial x} \right] + kGA\left(\dfrac{\partial u}{\partial x} - \theta \right) = \rho I \dfrac{\partial^2 \theta}{\partial t^2}
\end{cases}
\tag{1}
$$

where u and θ are the beam's transverse displacement and rotation, respectivetly, E is the Young's modulus, I the second moment of area, ρ the density of material, A the cross-sectional area, k a shear correction factor ($k = 5/6$ for rectangular sections), and G the shear modulus, L the length of the beam and δ is de Dirac delta function. According to Lee and Park [58], the dynamic equilibrium equation based on the principle of virtual work can be written as

$$
\int_0^L EI \frac{\partial \theta}{\partial x} \delta\left(\frac{\partial \theta}{\partial x} \right) dx + \int_0^L kGA\left(\frac{\partial u}{\partial x} - \theta \right) \delta\left(\frac{\partial u}{\partial x} - \theta \right) dx =
$$
$$
\int_0^L \delta u \rho A \ddot{u}\, dx + \int_0^L \delta\theta \rho I\, \ddot{\theta}\, dx + \int_0^L \delta\theta m_d\, \ddot{u}\, \delta\left(x - L_d \right) dx
\tag{2}
$$

which L the beam length and δ denotes the virtual terms. The equation of motion in the frequency domain in matrix form is given by

$$
\left| K - \omega_n^2 M \right| \Phi = 0
\tag{3}
$$

where Φ is a set of displacement-type amplitude at the control points otherwise known as the model vector, $f_n = \omega_n / 2\pi$ the natural frequency $[Hz]$, K and M are global stifness and mass matrices that can be explicitly written as:

$$
K = K_{ab} = \int_0^L \begin{bmatrix} 0 & -\dfrac{\partial N_{a,p}}{\partial x} \\ \dfrac{\partial N_{a,p}}{\partial x} & N_{a,p} \end{bmatrix}^T \begin{bmatrix} EI & 0 \\ 0 & kGA \end{bmatrix} \begin{bmatrix} 0 & -\dfrac{\partial N_{b,p}}{\partial x} \\ \dfrac{\partial N_{b,p}}{\partial x} & N_{b,p} \end{bmatrix} dx
\tag{4}
$$

$$
M = M_{ab} = \int_0^L N_{a,p} \rho A N_{a,p}\, dx + \int_0^L N_{a,p} \rho I N_{a,p}\, dx
\tag{5}
$$

where K_{ab} and M_{ab} are stiffness and mass matrices, respectively, to control points a and b; and $N_{a,p}$ and $N_{b,p}$ are the shape functions.

The elementary mass matrix M^e can be defined as consistent or concentrated. In the first case, it considers the acceleration effects in i and the inertia force in j. In other words, the mass matrix coefficients are not null when $i \neq j$. Briefly, to

determine M_{ij}^e a unitary acceleration is applied in the direction j. Thus, the inertia force that results in i is calculated to keep all the accelerations in other zero directions. Therefore, the consistent mass matrix is given by

$$M^e = \frac{\rho A L_e}{420} \begin{bmatrix} 156 & 22L_e & 54 & -13L_e \\ 22L_e & 4L_e & 13L_e & -3L_e^2 \\ 54 & 13L_e & 156 & -22L_e \\ -13L_e & -3L_e^2 & -22L_e & 4L_e^2, \end{bmatrix}$$ (6)

where L_e is the length of the element.

Dimensionless equation

The Timoshenko beam design is performed to determine dimensionless variables and the parameters that govern the problem. Considering the equilibrium equations of bending and shear moments (1) of a Timoshenko beam with constant section, the equation of motion is given by:

$$\begin{cases} \rho A \ddot{u} - kGA(u'' - \theta') = f \\ \rho I \ddot{\theta} - EI\theta'' - kGA(u' - \theta) = 0 \end{cases}$$ (7)

The second equation when taking derivatives with respect to space becomes

$$\rho I (\ddot{\theta})' - EI\theta''' \underbrace{- kGA(u'' - \theta')}_{= f - \rho A \ddot{u}} = 0$$ (8)

where ρ is the material density, A the cross-section area, u the transversal displacement, θ the rotation, k the shear correction factor, G the shear modulus, f the external force, I the second moment of area and E the Young's modulus. Then, Eqn. (8) can rewritten as,

$$\rho I (\ddot{\theta})' - EI\theta''' + f - \rho A \ddot{u} = 0$$ (9)

that is,

$$(EI\theta')'' + \rho A \ddot{u} - f - (\rho I \ddot{\theta})' = 0$$ (10)

where we can introduce $\theta' = u'' - \alpha'$. From this,

$$[EI(u'' - \alpha')]'' + \rho A \ddot{u} - f - (\rho I \ddot{\theta})' = 0$$ (11)

in which EI and ρA are constant. Thus,

$$EIu^{IV} - EI\alpha''' + \rho A \ddot{u} - f - \rho I \left(\ddot{u}'' - \ddot{\alpha}' \right) = 0$$ (12)

Recall that,

$$\rho A \ddot{u} - kGA(\alpha') = f$$ (13)

where $\alpha' = \dfrac{\rho}{kG}\ddot{u} - \dfrac{f}{kGA}$. In this way, the equation of motion can be expressed as follows

$$EIu^{IV} - \left(\frac{EI\rho}{kG} + \rho I\right)\ddot{u}'' + \rho A\ddot{u} + \frac{\rho^2 I}{kG}\ddddot{u} = f - \frac{EI}{kGA}f'' + \frac{\rho I}{kGA}\ddot{f} \tag{14}$$

Considering this is a problem of free vibration with mass addition as discontinuity m_d at L_d, we have

$$EIu^{IV} - \left(\frac{EI\rho}{kG} + \rho I\right)\ddot{u}'' + \rho A\ddot{u} + \frac{\rho^2 I}{kG}\ddddot{u} + m_d\ddot{u}\delta(x - L_d) = 0 \tag{15}$$

Assuming $u = \delta_x\bar{u}$, $x = L\bar{x}$ and $t = \dfrac{\overline{T}}{\overline{t}} = \dfrac{\overline{t}}{f_n}$ in which $\bar{u}$, $\bar{x}$, and $\overline{t}$ are dimensionless parameters, Eqn. (15) is given by

$$EI\frac{\delta_x}{L^4}\bar{u}^{IV} - \left(\frac{EI\rho}{kG} + \rho I\right)\frac{\delta_x}{L^2}f_n^2\ddot{\bar{u}}'' + \rho A\delta_x f_n^2\ddot{\bar{u}} + \frac{\rho^2 I}{kG}\delta_x f_n^4\ddddot{\bar{u}} + m_d\delta_x f_n^2\ddot{\bar{u}}\delta\left(\frac{x}{L_d} - 1\right) = 0 \tag{16}$$

Dividing everything by $\rho A\delta_x f_n^2$, Eqn. (16) is described as

$$\frac{EI}{\rho AL^4 f_n^2}\bar{u}^{IV} - \left(\frac{E}{kG} + 1\right)\frac{I}{A}\frac{1}{L^2}\ddot{\bar{u}}'' + \ddot{\bar{u}} + \frac{\rho^2 I}{kG}\frac{f_n^4}{\rho A f_n^2}\ddddot{\bar{u}} + \frac{m_d}{\rho A}\ddot{\bar{u}}\delta\left(\frac{x}{L_d} - 1\right) = 0 \tag{17}$$

Furthermore, according to Blevins [59]:

$$\frac{1}{\rho A f_n^2} = \frac{4\pi^2 L^4}{\beta^4 EI} \tag{18}$$

Thus, the equation of motion can be given by

$$\frac{4\pi^2}{\beta^4}\bar{u}^{IV} - \left(\frac{E}{kG} + 1\right)\frac{I}{A}\frac{1}{L^2}\ddot{\bar{u}}'' + \ddot{\bar{u}} + \frac{\rho f_n^2 I}{kGA}\ddddot{\bar{u}} + \frac{m_d}{\rho AL}\ddot{\bar{u}}\delta\left(\bar{x} - \frac{L_d}{L}\right) = 0 \tag{19}$$

It is known that $E/Gk = \kappa$ and $I/A = R^2$ (radius of rotation of the cross section), we have the dimensionless motion equation of the Timoshenko beam:

$$\frac{4\pi^2}{\beta^4}\bar{u}^{IV} - \underbrace{(\kappa + 1)R^2\frac{1}{L^2}\ddot{\bar{u}}''} + \ddot{\bar{u}} + \underbrace{\frac{\rho f_n^2 R^2}{kG}\ddddot{\bar{u}}} + \frac{m_d}{\rho AL}\ddot{\bar{u}}\delta\left(\bar{x} - \frac{L_d}{L}\right) = 0 \tag{20}$$

where $\delta = [1/L]$.

Neglecting the terms underlined in Eqn. (20), the dimensionless beam motion equation is obtained on the Euler-Bernoulli theory that considers a kinematic hypothesis formulated without considering the shear and the rotational beam effects. In Eqn. (21), the motion of the Euler-Bernoulli beam is described.

$$\frac{4\pi^2}{\beta^4}\bar{u}^{IV} + \ddot{\bar{u}} + \frac{m_d}{\rho AL}\ddot{\bar{u}}\delta\left(\bar{x} - \frac{L_d}{L}\right) = 0 \tag{21}$$

Therefore, it is noted that the behavior of the beam is a function of its boundary condition β, the intensity of the mass discontinuity m_d and its position L_d.

METHODOLOGY

Wavelet transforms

The one-dimensional wavelet transform projects a signal into two-dimensional space. Considering a signal $f(x)$, the wavelet transform is defined as

$$W_f^{\phi}(a,\iota) = |a|^{-\frac{1}{2}} \int_{-\infty}^{\infty}, f(x)\phi^*\left(\frac{x-\iota}{a}\right)dx \tag{22}$$

where $\phi^*(.)$ indicates the conjugate complex of $\phi(.)$. The translation parameter ι indicates the location of the rove wavelet window in the wavelet transform and the scale a indicates the width of the wavelet window. It is a mathematical operation that expands or compresses the signal.

To detect damages, large scales are used to ensure that the signals are dilated, to make easier the identification of discontinuities. Disregarding the average value of the function $\varphi(x)$, we have

$$\int_{-\infty}^{\infty}\phi(x)dx = 0 \tag{23}$$

The corresponding function for wavelet transform is given by

$$\phi^{a,\iota}(x) = |a|^{-\frac{1}{2}} \phi^*\left(\frac{x-\iota}{a}\right) \tag{24}$$

where $\phi^{a,\iota}$ is the generating (basis) functions in the spatial domain x from which the wavelet coefficients by translation and scale are generated. This function is also known as "mother wavelet".

Discrete wavelet transform

In the Discrete Wavelet Transform (DWT), the mother wavelet function can be generated by scale a and translation ι in powers of two. In this context, it reduces the computational cost in calculating the respective coefficients. The scale parameter is defined as 2^a and the translation 2^a. This way, the wavelet functions are given by

$$TDW_{a,\iota} = 2^{\frac{-a}{2}} \int_{-\infty}^{\infty} f(x)\phi\left(2^{-a}x - \iota\right)dx = \int_{-\infty}^{\infty} f(x)\phi_{a,\iota}(x)dx \tag{25}$$

where a and ι refers to the scale and translation parameters.

Palechor [15] presents four steps to damage detection from the DWT:

    1. obtain a signal associated with the complete structure's response or a specific area of the structure;
    2. compute the wavelet coefficients, performing the signal's DWT at different levels or different scales;
    3. plot the graph of the wavelet coefficients for each level of decomposition;
    4. analyze the distribution of the wavelet coefficients for each level.

A severe change (peak) in the distribution of the wavelet coefficients means a local disturbance. If the disturbance detected is not caused by a known source, such as geometric or material discontinuity, then this means that there is damage near to the location of the disturbance.

Wavelet damage ratio index

Four basis wavelet functions were tested in this work: db5, coif3, and sym6 and bior6.8. To define the most useful function to facilitate damage detection, it is proposed the wavelet damage ratio (WDR). This index is used to evaluate the damage level by the relation between the damage signal S_d and the base signal S_b:

$$WDR[dB] = 20 log_{10}\left(\frac{Sd}{Sb}\right) \qquad (26)$$

in which S_d corresponds to the damage position that is the maximum absolute value (peak) of the wavelet coefficients, desconsidering the high values in the ends caused by the geometric descontinuities of the beam and/or the boundary conditions. Thus, S_b consists of the maximum local value of the region without singularities, as shown in Fig. 1 that presents the plots using the four functions for each DWT calculated.
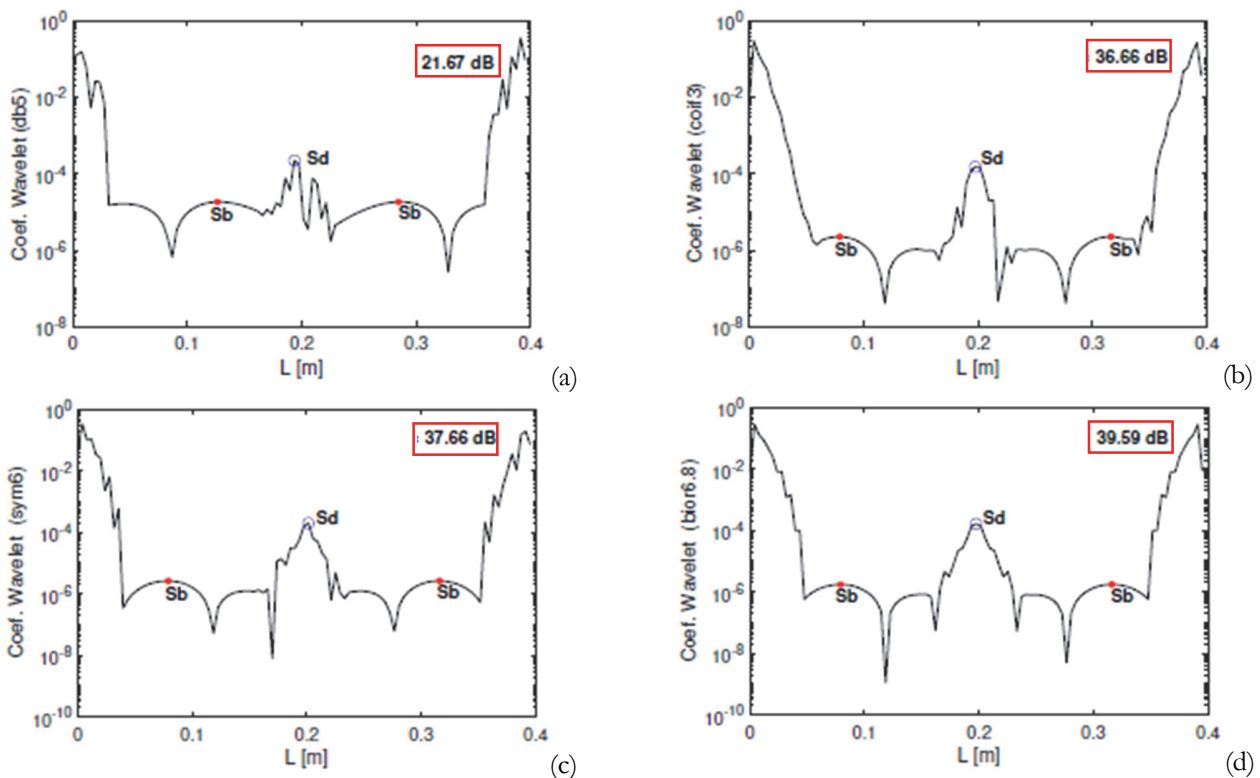

Figure 1: WDR index determination using the wavelet functions (a) db5; (b) coif3; (c) sym6; (d) bior6.8.

Fig. 1 refers to the free-free beam. By the way, the same procedure was carried out in a simply supported beam. In both situations, the bior6.8 function presented high values of WDR, showing more useful for damage detection in the Timoshenko beam by this technique.

NUMERICAL EXAMPLE

Numerical analyses of an aluminum beam were carried out using the parameters estimated experimentally in the Systems and Vibrations laboratory of the University of Brasília, UnB. Tab. 1 presents the geometric and material properties of the beam used as a reference for the present study.

Two different boundary conditions were applied: free-free (F-F) and supported-supported (S-S). Firstly, the damage was simulated as an additional mass positioned in different locations of the beam: L/2 and L/4. Fig. 2 presents the investigated cases.

Characteristics of the beam	
Mass [g]	385.33
Length [mm]	395.0
Base of the cross-section [mm]	19.0
Height of the cross-section [mm]	19.0
Cross section area [mm²]	361.00
Moment of inertia [mm⁴]	$1.086.10^{-4}$
Modulus of elasticity [GPa]	66.66
Shear modulus [GPa]	24.18
Density [kg/m³]	2702.27
Poisson's ratio	0.33

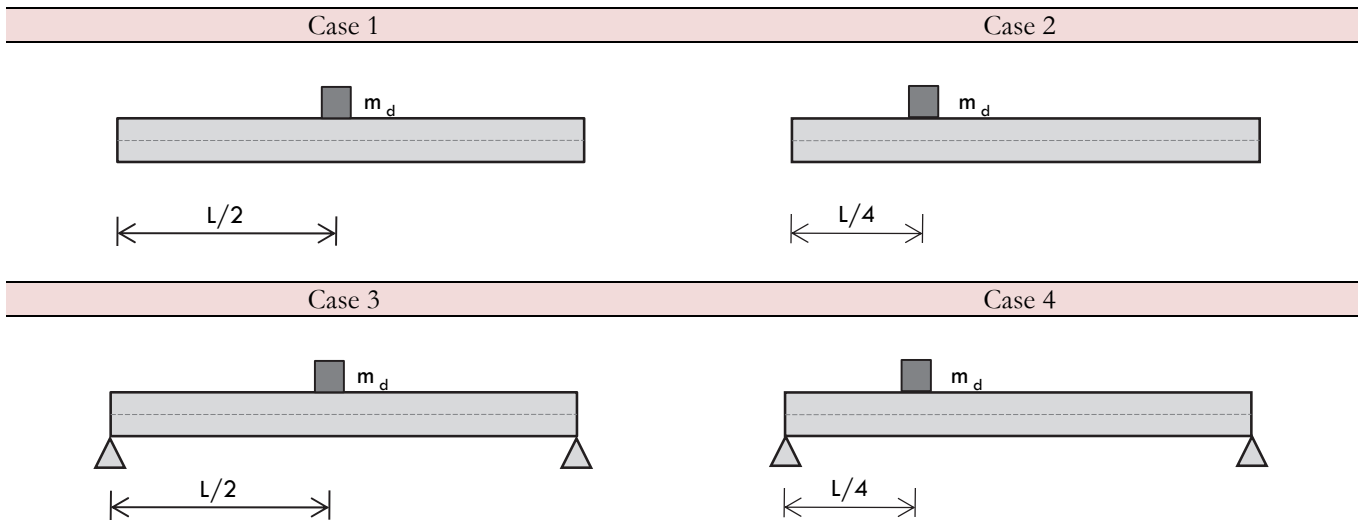Table 1: Geometric and material properties of the aluminum beam.

Figure 2: Beam cases with different boundary conditions and damage positions.

Frequency-Shift

The frequency-shift technique was used for the first three vibration modes of the cases. An additional roving mass m_a equal to 2% of the total beam mass was applied. The damage was modeled as an additional mass m_d varied from 1% to 5% of the beam total mass m_t. The beam was discretized into 100 elements for this analysis. The spatial evolution of the first three frequencies for the four cases is shown in Figs. 3-4.

In all cases, the sensitivity of natural frequencies is noted when an additional mass was applied along the beam length. Besides, the influence of the structure's mode shape was observed since the natural frequency curve undergoes minor variations when the damage is located at a nodal point, as shown in Fig. 3 (b1 and a2), and Fig. 4 (b1). Next, the influence of modes is presented in more detail.

DWT

A convergence analysis was performed for the example of free-free beam (C1) and simply supported beam (C3) case with mass discontinuity (Fig. 5). Several simulations were performed for 10, 50, 100 and 500 finite elements to evaluate DWT of frequency shift curve, using bior6.8 mother wavelet. For better visualization, only the DWT result was plotted for higher

intensity damage ($m_d = 5\% \, m_t$) and light mass additional ($m_d = 2\% \, m_t$). However similar results were obtained for all set of damage levels and mass additional.

The wavelet coefficients reach fully convergence for 500 finite elements. It is observed a tendency of improvement with damage severity. Therefore, for the present analysis, it is sufficient to use 100 finite elements to detect reasonably the damage position in the present cases with a considerable reduction of computational effort.

In experimental point of view, Palechor et al. [15] carried out the need to apply interpolation methods to increase the amount of data. Experimental data is limited to the number of points that can be measured with available instrumentation. To apply the Wavelet Transform, it became necessary to increase the discrete data to obtain good results in damage localization. The interpolation method used was the Cubic Spline, which, presented the best results in the identification of damage in metal beams under static tests according to Palechor et al. [60].
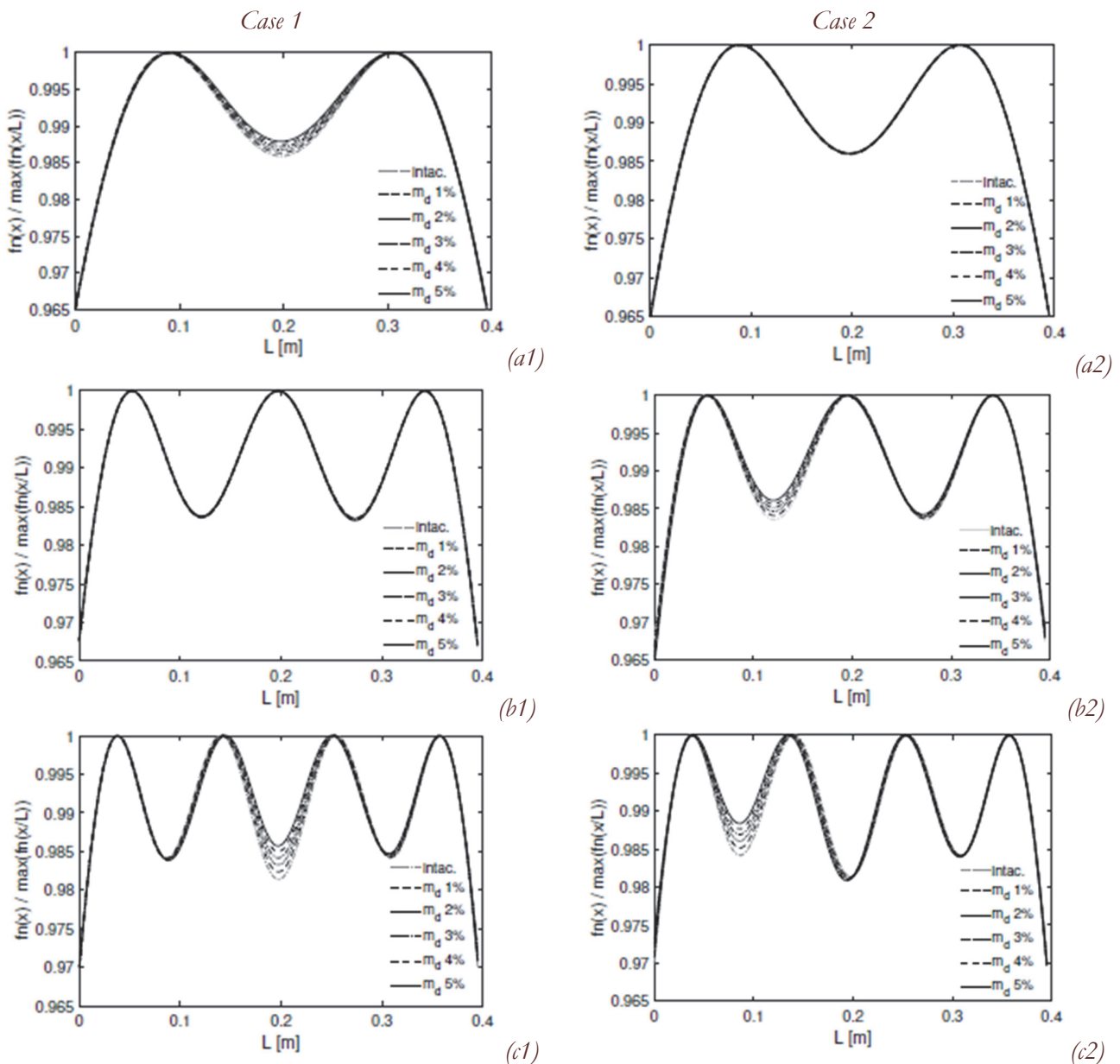

Figure 3: Frequency variation $f_n(x/L)/max \, (f_n(x/L))$ depending on the position of m_a in free-free beams (cases C1 and C2): (a) first frequency, (b) second frequency and (c) third frequency.
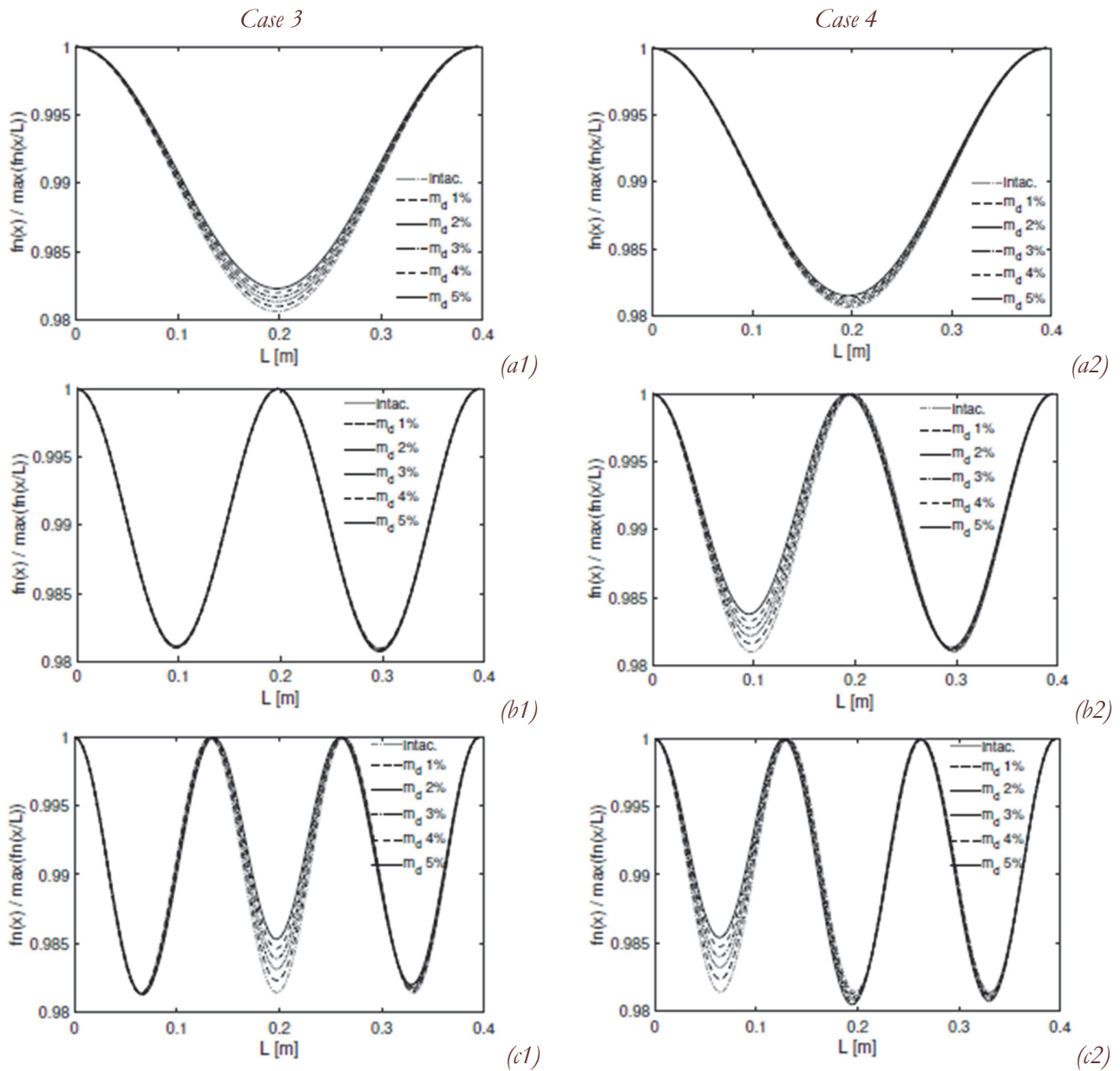
Figure 4: Frequency variation $f_n(x/L)/\max(f_n(x/L))$ depending on the position of m_a in simple supported beams (cases C3 and C4): (a) first frequency, (b) second frequency and (c) third frequency.

Roving mass (m_a) and damage mass (m_d) relation

Given a damage located in the center of free-free (C1) and simply supported (C3) beams, using the bior6.8 mother wavelet, the influence of the additional mass m_a on the frequency shift curve is studied. Figs. 6 and 7 present the frequency shift curve for 1 and 10% damage relative to roving masses of 1, 2 and 5% additional mass.

In the case of a free-free beam (C1), Fig. 6 presents a frequency shift curve for additional mass of 5% with a slight tendency to saturation. Fig. 7, for the simply supported case (C3), shows a clearer trend in this regard. In these cases, increasing the additional mass does not improve the perception of damage, that is, an increase in WDR.
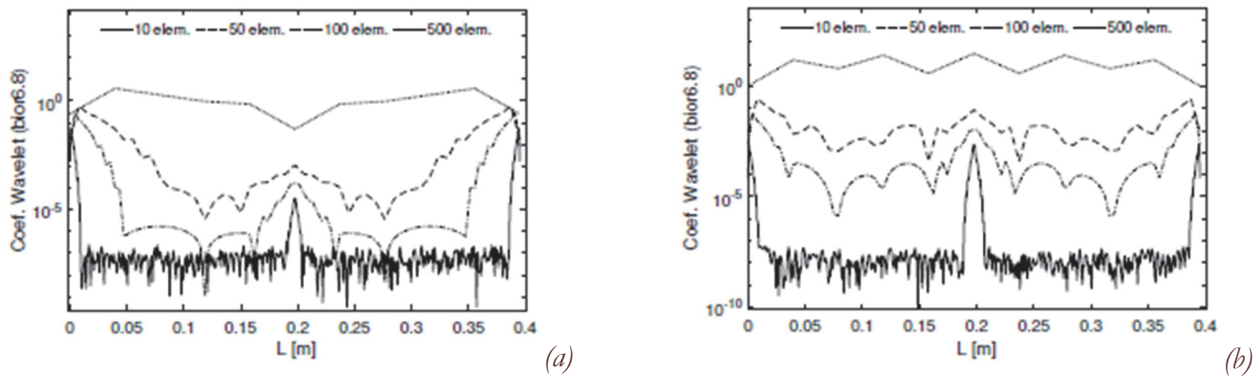
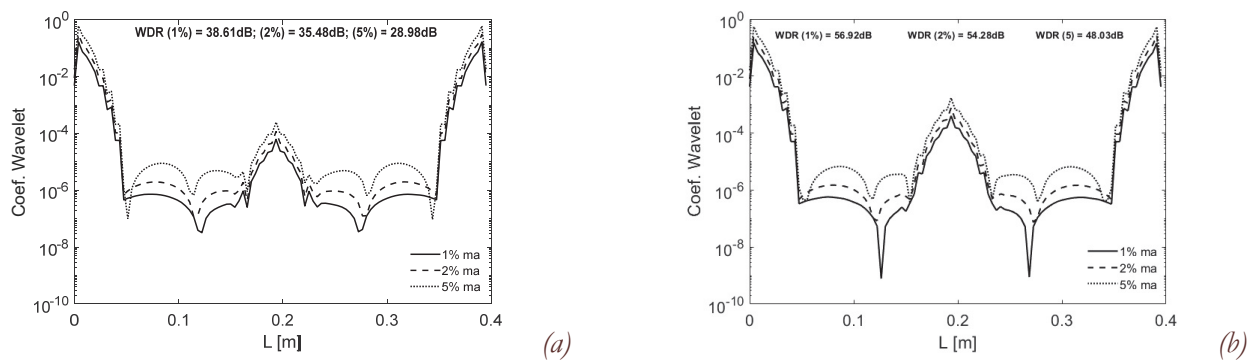Figure 5: Element convergence analysis of DWT of first frequency-shift curve in cases C1 (a) and C2 (b).

Figure 6: Frequency-shift curve of C1 beam as function of roving mass m_a for damage mass m_d of 1% (a) and 10% (b).
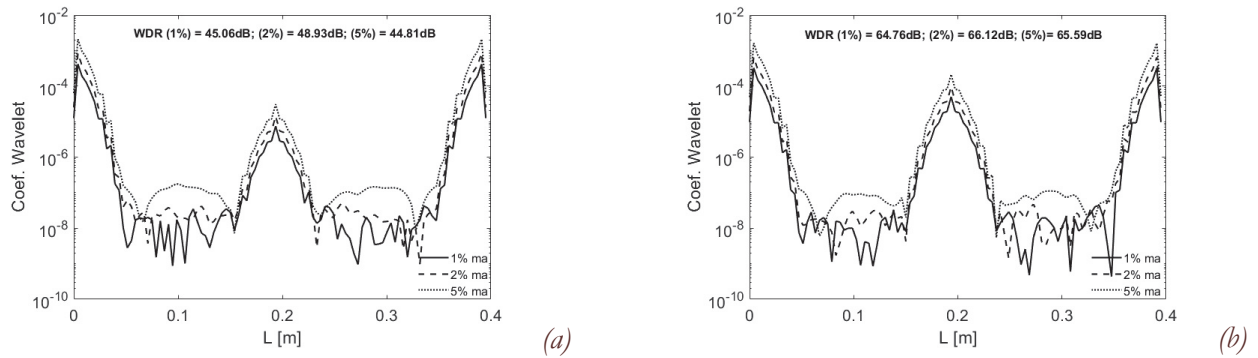

Figure 7: Frequency-shift curve of C3 beam as function of roving mass m_a for damage mass m_d of 1% (a) and 10% (b).

RESPONSE MAP AND DISCUSSION RESULTS

After Section Numerical Results, the presence of some dimensionless numbers is highlighted in Timoshenko beam dimensionless equation: additional moving mass ratio m_a, damage mass ratio m_d and the damage position x / L. The relationship between these variables and WDR was investigated. Figs. 8 and 9 present WDR for first and second natural frequency of free-free and simply supported beams, respectively, as a function of the ratio of damage mass and total mass m_d / m_T positioned at $1/8L$, $1/4L$, $3/8L$ and $1/2L$. The symmetry of beam was considered. The WDR response map is represented for half beam. For both figures, the roving mass is 1% of total mass.
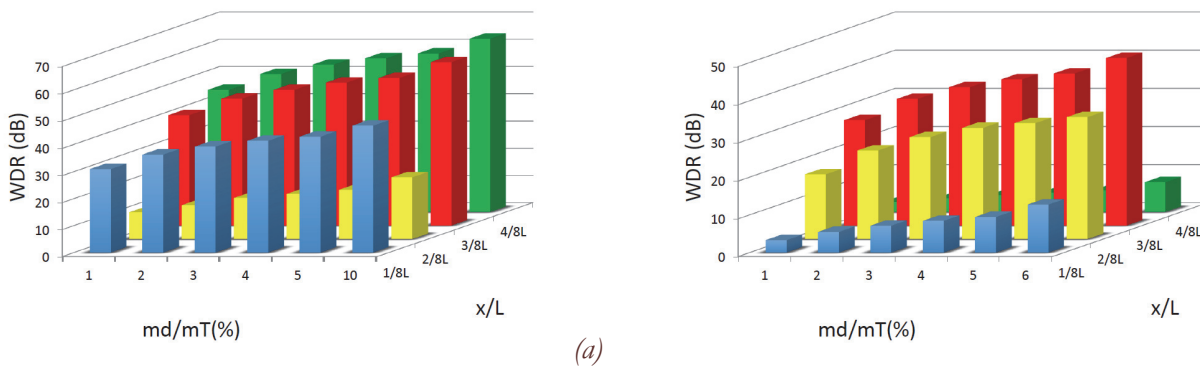
Figure 8: Response map of WDR (dB) of free-free (C1) beam as function of damage mass ratio m_d / m_T and position ratio x / L for 1st (a) and 2nd (b) frequencies and roving mass m_a of 1%.
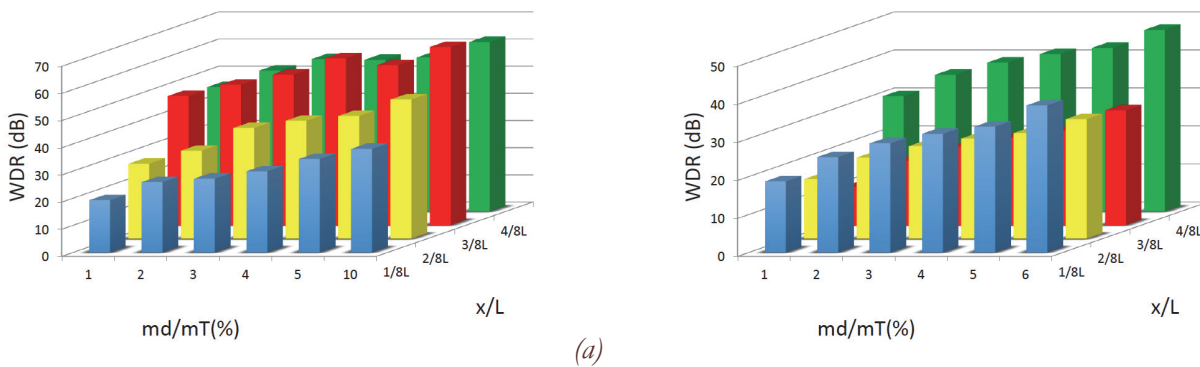

Figure 9: Response map of WDR (dB) of simply supported (C3) beam as function of damage mass ratio m_d / m_T and position ratio x / L for 1st (a) and 2nd (b) frequencies and roving mass m_a of 1%.

WDR response maps show the influence of damage mass (for a specific roving mass) and damage position for damage localization's frequency-shift technique for Timoshenko beams in free-free and simply support boundary conditions. Fig. 8a shows a WDR reduction at $2/8L(0.250L)$, i.e., closer to a nodal point for first modal shape of free-free beam. The similar reduction for second modal shape for free-free beam is observed at $1/8L(0.125L)$ and $4/8L(0.500L)$. Fig. 9 shows better results of WDR for damage mass located at middle span for the simply supported beam.

The index WDR associated with roving mass technique can be used as a metric to determine and to localize damage in beam-like structures. Associate to machine learning techniques, the interpretation of wavelet transform of frequency shift function can be automatized to be used as a damage index. However, more studies are necessary to be done.

CONCLUSIONS

This research paper presented a numerical study of additional mass spatial probing identification technique using discrete wavelet transforms of frequency shift curves of damaged Timoshenko FE 2-nodes beam. It was used a mass discontinuity to simulation damage, known as damage mass. Using a roving mass positioned along beam span, a modal frequency was monitored to determine the frequency-shift curve. And the discrete wavelet transform of the frequency-shift curve are used to locate the damage. Simply supported and free-free beams was analyzed for two damage mass, ¼ and ½ of beam span. WDR index is proposed to analyze the magnitude of the damage. Also, it was evaluated for different levels and positions of damages, and it was presented as maps.

The frequency-shift curve makes it possible to detect and locate a damage using only damaged response, eliminating comparison to an intact response. The WDR index proposed a metric to reduce frequency-shift curve as a value. With WDR, a response map synthetizing the level of damage was produced. The node of modal shape has an influence in damage

detection for a determined modal frequency. This point-out to necessity to analyses more than one frequency for a good damage detection procedure using frequency-shift curve.

Other essays are necessary to correlate mass discontinuity with damage and make a relationship of damage deep for open cracks. Numerical and experimental studies are necessary associating the frequency-shift technique to mobile roving mass, as a vehicle, to allow the monitoring of bridges in a more agile way. And a more detailed analysis of the influence of noise is suggested for future works.

REFERENCES

[1] Rytter, A. (1993).Vibrational Based Inspection of Civil Engineering Structures. Aalborg Universitet.

[2] Khedmatgozar Dolati, S.S., Caluk, N., Mehrabi, A., Khedmatgozar Dolati, S.S. (2021). Non-Destructive Testing Applications for Steel Bridges, Appl. Sci., 11(20), pp. 9757, DOI: 10.3390/app11209757.

[3] Uesaka, M., Mitsuya, Y., Dobashi, K., Kusano, J., Yoshida, E., Oshima, Y., Ishida, M. (2018). On-Site Bridge Inspection by 950 keV/3.95 MeV Portable X-Band Linac X-Ray Sources, Bridg. Optim. - Insp. Cond. Monit.,
DOI: 10.5772/INTECHOPEN.82275.

[4] Salgado, R. (2008). Damage Detection Methods in Bridges through Vibration Monitoring: Evaluation and Application, pp. 289.

[5] Sun, H., Wang, T., Lin, D., Wang, Y., Qing, X. (2020). An Eddy Current-Based Structural Health Monitoring Technique for Tracking Bolt Cracking, Sensors (Basel). 20(23), pp. 1–14, DOI: 10.3390/S20236843.

[6] Moore, P.O., Moore, D.G. (2016). Nondestructive testing handbook. 1, Liquid penetrant testing, American Society for Nondestructive Testing.

[7] Nair, A., Cai, C.S. (2010). Acoustic emission monitoring of bridges: Review and case studies, Eng. Struct., 32(6), pp. 1704–1714, DOI: 10.1016/j.engstruct.2010.02.020.

[8] Amezquita-Sanchez, J.P., Adeli, H. (2016). Signal Processing Techniques for Vibration-Based Health Monitoring of Smart Structures, Arch. Comput. Methods Eng., 23(1), pp. 1–15, DOI: 10.1007/s11831-014-9135-7.

[9] Hou, R., Xia, Y. (2021). Review on the new development of vibration-based damage identification for civil engineering structures: 2010–2019, J. Sound Vib., 491, pp. 115741, DOI: 10.1016/J.JSV.2020.115741.

[10] Parloo, E., Vanlanduit, S., Guillaume, P., Verboven, P. (2004). Increased reliability of reference-based damage identification techniques by using output-only data, J. Sound Vib., 270(4–5), pp. 813–832,
DOI: 10.1016/S0022-460X(03)00494-2.

[11] Duan, Z., Yan, G., Ou, J., Spencer, B.F. (2005). Damage localization in ambient vibration by constructing proportional flexibility matrix, J. Sound Vib., 284(1–2), pp. 455–466, DOI: 10.1016/J.JSV.2004.06.046.

[12] Zhong, S., Oyadiji, S.O., Ding, K. (2008). Response-only method for damage detection of beam-like structures using high accuracy frequencies with auxiliary mass spatial probing, J. Sound Vib., 311(3–5), pp. 1075–1099,
DOI: 10.1016/j.jsv.2007.10.004.

[13] Palechor, E.U.L., Silva, R.S.Y.C., Bezerra, L.M., Bittencourt, T.N. (2014). Damage Identification in Beams Using Experimental Data, Key Eng. Mater., 607, pp. 21–29, DOI: 10.4028/www.scientific.net/KEM.607.21.

[14] Silva, R.S.Y.R.C., Palechor, E.U.L., Bezerra, L.M., de Morais, M.V.G., da Silva, W. V. (2019). Damage detection in a reinforced concrete bridge applying wavelet transform in experimental and numerical data, Frat. Ed Integrità Strutt., 13(48), pp. 693–705, DOI: 10.3221/IGF-ESIS.48.65.

[15] Palechor, E.U.L., Bezerra, L.M., Morais, M.V.G. de., Silva, R., Barros, E. (2019). Damage identification in beams using additional rove mass and wavelet transform, Frat. Ed Integrità Strutt., 13(49), pp. 614–29,
DOI: 10.3221/IGF-ESIS.49.56.

[16] Silva, R.S.Y.C., Bezerra, L.M., Brito, M.A.N. (2012). Determination of damages in beams using wavelet transforms, Lect. Notes Eng. Comput. Sci., 2198, pp. 1211–1213.

[17] Carden, E.P., Fanning, P. (2004). Vibration Based Condition Monitoring: A Review, Struct. Heal. Monit., 3(4), pp. 355–377, DOI: 10.1177/1475921704047500.

[18] Montalvao, D., Maia, N.M.M., Ribeiro, A.M.R. (2006). A Review of Vibration-based Structural Health Monitoring with Special Emphasis on Composite Materials, Shock Vib. Dig., 38(4), pp. 295–324, DOI: 10.1177/0583102406065898.

[19] Fan, W., Qiao, P. (2011). Vibration-based Damage Identification Methods: A Review and Comparative Study, Struct. Heal. Monit., 10(1), pp. 83–111, DOI: 10.1177/1475921710365419.

[20] Cornwell, P., Doebling, S.W., Farrar, C.R. (1999). Application of the strain energy damage detection method to plate-like structures, J. Sound Vib., 224(2), pp. 359–374, DOI: 10.1006/jsvi.1999.2163.

[21] Shi, Z.Y., Law, S.S., Zhang, L.M. (2000). Structural Damage Detection from Modal Strain Energy Change, J. Eng. Mech., 126(12), pp. 1216–1223, DOI: 10.1061/(ASCE)0733-9399(2000)126:12(1216).

[22] Hu, H., Wang, B.-T., Lee, C.-H., Su, J.-S. (2006). Damage detection of surface cracks in composite laminates using modal analysis and strain energy method, Compos. Struct., 74(4), pp. 399–405, DOI: 10.1016/j.compstruct.2005.04.020.

[23] Hu, H., Wu, C. (2009). Development of scanning damage index for the damage detection of plate structures using modal strain energy method, Mech. Syst. Signal Process., 23(2), pp. 274–287, DOI: 10.1016/j.ymssp.2008.05.001.

[24] Yan, W.-J., Huang, T.-L., Ren, W.-X. (2010). Damage Detection Method Based on Element Modal Strain Energy Sensitivity, Adv. Struct. Eng., 13(6), pp. 1075–1088, DOI: 10.1260/1369-4332.13.6.1075.

[25] Seyedpoor, S.M. (2012). A two stage method for structural damage detection using a modal strain energy based index and particle swarm optimization, Int. J. Non. Linear. Mech., 47(1), pp. 1–8, DOI: 10.1016/j.ijnonlinmec.2011.07.011.

[26] Amiri, M., Zangeneh, B.N. (2008).Structural damage identification using modal strain energy method. 8th International Congress of Coasts, Ports and Marine Structures, Tehran, Iran, pp. 2599–2607.

[27] Cha, Y.-J., Buyukozturk, O. (2015). Structural Damage Detection Using Modal Strain Energy and Hybrid Multiobjective Optimization, Comput. Civ. Infrastruct. Eng., 30(5), pp. 347–358, DOI: 10.1111/mice.12122.

[28] Ashory, M.-R., Ghasemi-Ghalebahman, A., Kokabi, M.-J. (2018). An efficient modal strain energy-based damage detection for laminated composite plates, Adv. Compos. Mater., 27(2), pp. 147–162,
DOI: 10.1080/09243046.2017.1301069.

[29] Wang, S., Xu, M. (2019). Modal Strain Energy-based Structural Damage Identification: A Review and Comparative Study, Struct. Eng. Int., 29(2), pp. 234–248, DOI: 10.1080/10168664.2018.1507607.

[30] Hao, H., Xia, Y. (2002). Vibration-based Damage Detection of Structures by Genetic Algorithm, J. Comput. Civ. Eng., 16(3), pp. 222–229, DOI: 10.1061/(ASCE)0887-3801(2002)16:3(222).

[31] Laier, J.E., Morales, J.D. V. (2009).Improved Genetic Algorithm for Structural Damage Detection. Computational Structural Engineering, Dordrecht, Springer Netherlands, pp. 833–839.

[32] Meruane, V., Heylen, W. (2010). Damage Detection with Parallel Genetic Algorithms and Operational Modes, Struct. Heal. Monit., 9(6), pp. 481–496, DOI: 10.1177/1475921710365400.

[33] Meruane, V., Heylen, W. (2011). An hybrid real genetic algorithm to detect structural damage using modal properties, Mech. Syst. Signal Process., 25(5), pp. 1559–1573, DOI: 10.1016/j.ymssp.2010.11.020.

[34] Aktasoglu, S., Sahin, M. (2012).Damage Detection in Beam Structures using a Combined Genetic Algorithm and Nonlinear Optimisation System. Civil-Comp Proceedings, vol. 99, Civil-Comp Press.

[35] Behera, S. R., Parhi, D. C., Das, H. (2018). Application of genetic algorithm for crack diagnosis of a free-free aluminum beam with transverse crack subjected to axial and bending load, J. Mech. Eng. Sci., 12(3), pp. 3825–3851,
DOI: 10.15282/jmes.12.3.2018.6.0337.

[36] Krawczuk, M. (2002). Application of spectral beam finite element with a crack and iterative search technique for damage detection, Finite Elem. Anal. Des., 38(6), pp. 537–548, DOI: 10.1016/S0168-874X(01)00084-1.

[37] Palacz, M., Krawczuk, M. (2002). Analysis of longitudinal wave propagation in a cracked rod by the spectral element method, Comput. Struct., 80(24), pp. 1809–1816, DOI: 10.1016/S0045-7949(02)00219-5.

[38] Su, Z., Ye, L. (2009). Identification of Damage Using Lamb Waves, 48, London, Springer London.

[39] Raghavan, A., Cesnik, C.E.S. (2007). Review of Guided-wave Structural Health Monitoring, Shock Vib. Dig., 39(2), pp. 91–114, DOI: 10.1177/0583102406075428.

[40] Chondros, T.G., Dimarogonas, A.D. (1980). Identification of cracks in welded joints of complex structures, J. Sound Vib., 69(4), pp. 531–538, DOI: 10.1016/0022-460X(80)90623-9.

[41] Salawu, O.S. (1997). Detection of structural damage through changes in frequency: A review, Eng. Struct., 19(9), pp. 718–723, DOI: 10.1016/S0141-0296(96)00149-6.

[42] Zhong, S., Oyadiji, S.O. (2008). Analytical predictions of natural frequencies of cracked simply supported beams with a stationary roving mass, J. Sound Vib., 311(1–2), pp. 328–352, DOI: 10.1016/j.jsv.2007.09.009.

[43] Zhong, S., Oyadiji, S.O. (2008). Identification of cracks in beams with auxiliary mass spatial probing by stationary wavelet transform, J. Vib. Acoust. Trans. ASME, DOI: 10.1115/1.2891242.

[44] Palechor, E.U.L., Bezerra, L.M., Morais, M.V.G. de., Silva, R.S.Y.R.C. (2018). Identificação De Danos Em Vigas Metálicas Utilizando Massas Itinerantes Adicionais, Análise Experimental., Rev. Sul-Americana Eng. Estrutural, 15(3),
DOI: 10.5335/rsaee.v15i3.7886.

[45] Palechor, E.U.L., Machado, M.R., de Morais, M.V.G., Bezerra, L.M. (2018). Dynamic Analysis of a Beam with Additional Auxiliary Mass Spatial Via Spectral Element Method, Springer Proc. Math. Stat., 249, pp. 279–289,
DOI: 10.1007/978-3-319-96601-4_25/COVER/.

[46] Mahmoud, M.A., Abou Zaid, M.A. (2002). Dynamic response of a beam with a crack subject to a moving mass, J. Sound

Vib., 256(4), pp. 591–603, DOI: 10.1006/jsvi.2001.4213.

[47] Eun, H.-C., Park, S.-Y., Kim, R.-J. (2013).Damage detection of shear building structure based on FRF response variation. Current Research on Material, Architecture and Civil Engineering, vol. 32, Science & Engineering Research Support Society, pp. 18–25.

[48] Solís, M., Ma, Q., Galvín, P. (2018). Damage detection in beams from modal and wavelet analysis using a stationary roving mass and noise estimation, Strain, 54(2), pp. e12266, DOI: 10.1111/str.12266.

[49] Wang, L., Lie, S.T., Zhang, Y. (2016). Damage detection using frequency shift path, Mech. Syst. Signal Process., 66–67, pp. 298–313, DOI: 10.1016/j.ymssp.2015.06.028.

[50] Lee, E.-T., Eun, H.-C. (2015). Damage Detection Using Measurement Response Data of Beam Structure Subject to a Moving Mass, Lat. Am. J. Solids Struct., 12(12), pp. 2384–2402, DOI: 10.1590/1679-78251975.

[51] Silva, R.S.Y.R.C., Bezerra, L.M., Peña, L.A.P., Gomes, G., da Silva, W. (2019). Boundary element and wavelet transform methods for damage detection in 2D structures, Int. J. Comput. Methods Eng. Sci. Mech., 20(3), pp. 242–255, DOI: 10.1080/15502287.2019.1631407.

[52] Monaco, E., Franco, F., Lecce, L. (2000). Experimental and Numerical Activities on Damage Detection Using Magnetostrictive Actuators and Statistical Analysis, J. Intell. Mater. Syst. Struct., 11(7), pp. 567–578, DOI: 10.1106/2URV-D0HY-0QLA-HAWH.

[53] Papatheou, E., Manson, G., Barthorpe, R.J., Worden, K. (2014). The use of pseudo-faults for damage location in SHM: An experimental investigation on a Piper Tomahawk aircraft wing, J. Sound Vib., 333(3), pp. 971–990, DOI: 10.1016/j.jsv.2013.10.013.

[54] Tibaduiza, D., Torres-Arredondo, M.Á., Vitola, J., Anaya, M., Pozo, F. (2018). A Damage Classification Approach for Structural Health Monitoring Using Machine Learning, Complexity, 2018, pp. 1–14, DOI: 10.1155/2018/5081283.

[55] Mehrjoo, M., Khaji, N., Ghafory-Ashtiany, M. (2014). New Timoshenko-cracked beam element and crack detection in beam-like structures using genetic algorithm, Inverse Probl. Sci. Eng., 22(3), pp. 359–382, DOI: 10.1080/17415977.2013.788170.

[56] Friedman, Z., Kosmatka, J.B. (1993). An improved two-node timoshenko beam finite element, Comput. Struct., 47(3), pp. 473–481, DOI: 10.1016/0045-7949(93)90243-7.

[57] Ferreira, A.J.M. (2009). MATLAB Codes for Finite Element Analysis, 157, Dordrecht, Springer Netherlands.

[58] Lee, S.J., Park, K.S. (2013). Vibrations of Timoshenko beams with isogeometric approach, Appl. Math. Model., 37(22), pp. 9174–9190, DOI: 10.1016/j.apm.2013.04.034.

[59] Blevins, R.D. (2016). Formula for Dynamics, Acoustics, and Vibration, II, Willey.

[60] Palechor, E.U.L. (2013).Damage Identification in Steel Beams by Wavelets and Numerical/Experimental Signal (por. Identificação de Danos em Vigas Metálicas Utilizando Wavelets e Dados Numéricos e Experimentais). Universidade de Brasília.